### 1.2.8 WP 8 – Instrumentation – e-tools

The overall, common goal of the WP is to increase the availability and utilisation of the future ESS instruments. This will be achieved by advances in simulation methods (Task 8.1), shielding approaches (Task 8.2) and through development of "plugin" Larmor technology for selected instruments (Task 8.3).

The WP8 partners have shared ideas and results at multiple workshops and meetings, including:

- "Neutrons: Cradle to Grave workshop, Coimbra, Portugal, September 6th 2016" in connection with the first SINE2020 General Assembly (8 presentations, 15 participants).
- ICANS 2017 was attended by several partners and WP 8 had good visibility with 5 presentations and 2 posters.
- A sattelite WP meeting in connection with the ICANS conference in Oxford, April 2017.
- Multiple coordinating Skype meetings

**Task 8.1: E-tools for integrated simulation using neutronics and Monte Carlo ray-tracing** *(Responsible: DTU, Partners: PSI, ESS,NPI, ESS-Bilbao and MTA-EK)*

The task is developing software E-tools for *integrated simulation* using neutronics and Monte Carlo ray-tracing, i.e. will implement and assess new e-science tools for very accurate simulation of neutron beam-lines.

The activity brings together experts from both (a) neutronics, e.g. MCNP used for simulating production and transport of neutrons from the target (including high-energy neutrons and other particles) through moderators and reflectors and (b) Monte Carlo ray-tracing, e.g. McStas and RESTRAX, which in the range of cold and thermal neutrons can describe transport along guides and neutron interaction with other optical elements and samples.

The combination of these two types of code is necessary to allow optimising instruments and experiments from the source to the sample, including shielding. Including shielding allows estimating background, thereby increasing realism of instrument simulations – and for the first time express *instrumental signal to noise* by simulation techniques.

**Deliverable D8.2 – *Improved code interface, pre-release*** *(DTU, ESS and PSI)*

In synergy with the BrightnESS project (grant agreement No 676548), the task has developed a new, easy to use particle interchange format called *Monte Carlo Particle Lists* (MCPL) which allows transfer of simulated particle data between key simulation softwares applied in the design of the ESS facility and instruments, including MCNP, Geant4 and McStas.

MCPL allows describing all relevant parameters of standard model particles, and includes Portable C code for file manipulation plus converters and plugins for several popular simulation packages.

The software is released under the open-source *Creative Commons* CC0 license, available through the GitHub website, (https://mctools.github.io/mcpl/) and is further included in recent McStas software releases (2.4 and 2.4.1). An very comprensive documentation is available through the open access, peer-reviewed publication T. Kittelmann et.al., *Monte Carlo Particle Lists: MCPL* in Computer Physics Communications **218**, September 2017, pp 17–42 (https://doi.org/10.1016/j.cpc.2017.04.012). An

illlustration from the publication showing a small-angle neutron scattering (SANS) pattern from McStas, plus added realism from a subsequent Geant4 detector simulation is reproduced in the below Figure 1.

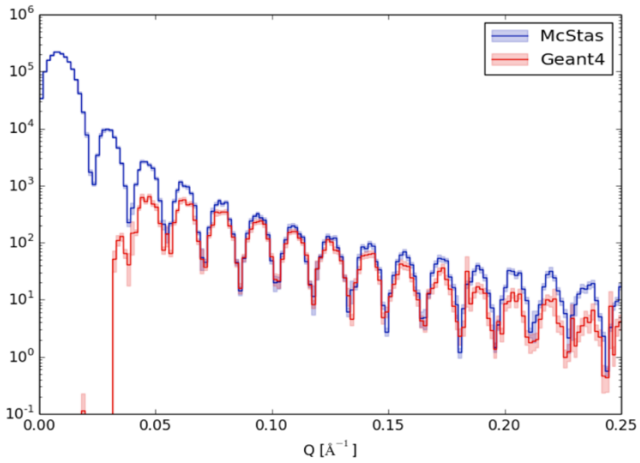


*Figure 1: reproduced from T. Kittelmann et. al.: Illustration of MCPL capabilities. A Geant4 detector simulation of the ESS LOKI Band-Gem detector added to post-sample output from McStas*

**Milestone workshop MS2: "*Neutrons: Cradle to Grave*"** *(All partners)*

The WP8 partners held the milestone workshop "Neutrons: Cradle to Grave workshop, Coimbra, Portugal, September 6th 2016" in connection with the first SINE2020 General Assembly. The workshop discussed different *variance reduction* schemes and methods applied in simulation tools from neutronics and Monte Carlo ray-tracing and how these can be shared and implemented between the different software codes. Figure 2 shows a photo of the participants in a coffee break.

As an example, the implementation of *bidirectional* neutron transport as implemented in the codes CombLayer and RESTRAX, and how these can be transferred to McStas was discussed. Also, possible variance-reduction solutions to the challenge of simulating long beamlines with neutronics codes were discussed, including the use of the ADVANTG (ORNL/TM-2013/416) and CombLayer (pp. 148-154 in JAEA-Conf 2015-002) methods.

All talks from the meeting were recorded and are available for viewing at http://coimbra2016.essworkshop.org/.

*Figure 2: A photo from one of the "Neutrons: Cradle to Grave" workshop coffee breaks*

**Work in progress toward Deliverable 8.8/8.11/8.12 -** (NPI)

At the above-mentioned workshop, results from NPI on interoperability and feature-exchange between RESTRAX and McStas was reported. Here we will only mention a highlight, namely the development of McStas-components for allowing a "reverse direction" simulation, i.e. from sample to source. This method has been available for a long time in RESTRAX, and is statistically much more efficient, as illustrated in Figure 3 below.

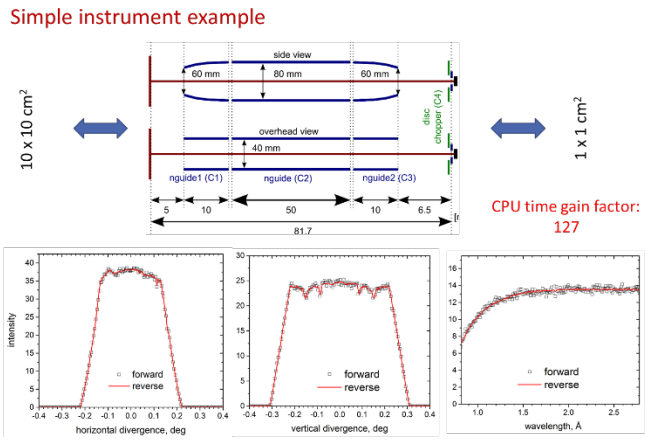


BEER@ESS: test with γ-Fe sample (Fe_Gamma.laz)

Conditions:

| | |
|---|---|
| *cylindrical sample*: | 7 x 20 mm² |
| *input slit*: | 5 x 10 mm², 50 mm before the sample |
| *output radial collimator*: | 4 mm resolution (*fwhm*) |
| *resolution mode*: | medium, $\Delta d/d$=0.3% |
| *detector coverage*: | $2\theta$ = 75° – 105°, $\phi$ = ± 15° |

*Simulation statistics (counts at the sample)*

| | forward | reverse | gain factor |
|---|---|---|---|
| Trials / $10^6$ | 5000 | 500 | |
| Counts / $10^6$ | 0.18 | 24 | |
| Efficiency [%] | 0.0037 | 4.7 | 1300 |
| Accuracy [%] | 0.34 | 0.031 | |
| Time [h] | 11.95 | 4.15 | |
| Time to 0.3 % accuracy [h] (*) | 9.2 | 0.045 | **200** |

(*) corresponds to about 20 000 counts in the strongest peak, using SPLIT 20

NOTE: The gain would be much higher for high resolution setup with small gauge volume of ~ 10 mm³ (typical for strain mapping experiments)

*Figure 3, From Jan Šaroun's presentation, Coimbra 2016. Left: Illustration of equivalence in simple forward and reverse simulation using McStas, demonstrating speed gain factor of 127. Right: The same approach is utilised in a more complicated virtual experiment simulation for the ESS BEER instrument, and an overall simulation speedup of 200 is found!*

Since the Coimbra meeting, NPI has been working on an MCPL (see D8.1 above) interface for RESTRAX/SIMRES, which will be presented in a poster at the ICNS conference in Korea in July 2017. The below Figure 4 shows a combined SIMRES-McStas simulation for the future BEER engineering diffractometer at the ESS. The reverse-direction capabilities of SIMRES provides a fast and statistically efficient primary spectrometer, combined with a realistic experimental-quality output from a PowderN

sample in the secondary spectrometer, defined in McStas.

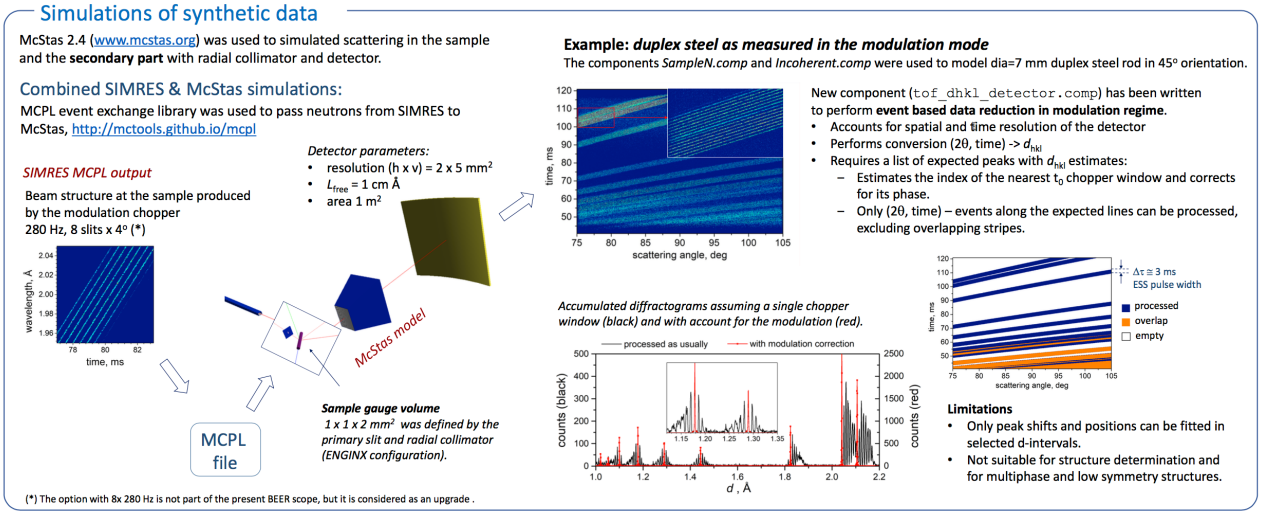


*Figure 4: RESTRAX/SIMRES now also has an MCPL interface, used in the figure for a combined simulation of the diffractometer BEER@ESS with McStas. The reverse-direction capabilities of SIMRES provides a fast and statistically efficient primary spectrometer, combined with a secondary spectrometer in McStas including the experimentally validated PowderN sample.*

**Task 8.2: Innovative Shielding Concepts and Materials** *(Responsible: PSI, Partners: ESS, STFC, ESS-Bilbao, TUM, MTA-EK and DTU)*

The task is enhancing understanding of high-energy neutron background at spallation sources, and optimising biological shielding through the development of new materials. The activity combines detailed, fast neutron background measurements at PSI and ISIS, which will be carried out using procedures common in the high-energy physics community and confronted with simulations. This work will lead to better neutron instrument design with lower fast neutron background. The development of new shielding materials could potentially also reduce the costs of neutron instruments since, nowadays, shielding constitutes an important fraction of an instrument budget. The new concepts will be tested at PSI on the BOA beamline, and at ISIS on the ChipIR beamline, before being more widely deployed.

**Deliverable 8.1 - Evaluation of detectors for fast neutron and gamma spectroscopy** (PSI)

PSI has performed an extensive evaluation of detector systems for characterising neutron backgrounds, the result of which can be found the D8.1 report. A performance study at four different spectrometer types found that the so-called Bonner Sphere Spectrometer (BSS) is superior, see Table 1

The BSS system is composed of a set of moderating polyethylene (PE) spheres of varying radius, each selected to moderate a characteristic high-energy neutron range to a region that can be measured by a standard He-3 counter inside the sphere. The only limitation of the system is that the upper energy response limit is around 20 MeV for a standard system based on PE spheres. To overcome this it was decided to attempt extension of the workable range by use of other materials (Pb, Cu). Figure 5 below contains an illustration of the BSS system and the extended energy range reached by the developed Cu and Pb inclusions.

| Type | Energy range | Energy resolution | Comments |
|---|---|---|---|
| Recoil proportional counter | 0.05 – 5 MeV | 10 % | limited energy range<br>high complexity for the detector system<br>high gamma ray sensitivity<br>pulse height analysis |
| Organic scintillator | 2-150 MeV | 4 % | limited energy range<br>high gamma ray sensitivity<br>pulse height analysis |
| Multisphere system<br>(BSS) | $10^{-8}$ – 20 MeV | > 10 % | wide energy range<br>extendable<br>mobil & easy to use<br>unfolding procedure |
| Foil radioactivation | 0.2 – 20 MeV | > 20 % | high neutron flux needed<br>limited energy range<br>low gamma response<br>unfolding procedure |

*Table 1: Properties of stuided spectrometer types, from D8.1 report*

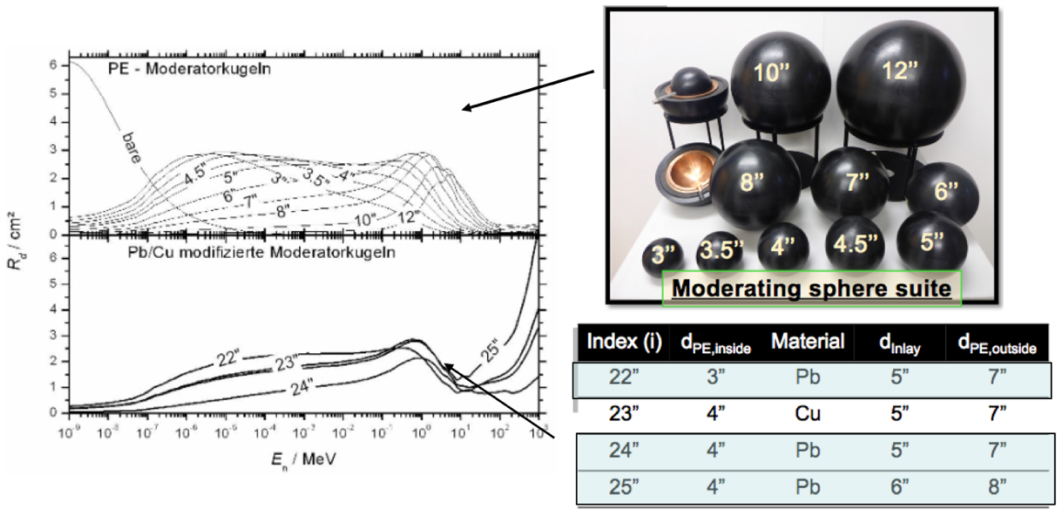


| Index (i) | $d_{PE,inside}$ | Material | $d_{Inlay}$ | $d_{PE,outside}$ |
|---|---|---|---|---|
| 22" | 3" | Pb | 5" | 7" |
| 23" | 4" | Cu | 5" | 7" |
| 24" | 4" | Pb | 5" | 7" |
| 25" | 4" | Pb | 6" | 8" |

*Figure 5: From Coimbra 2016 presentations by Uwe Filges, PSI. Shows how the PSI Bonner Sphere spectrometer has been supplemented with Pb/Cu moderating spheres, for extension of the dynamic range*

The neutron detector selected for use with the BSS spectrometer is a He-3 proportional counter from Centronic, type SP9/152/Kr/0916-21 (B). As part of D8.1 the detector efficiency has been measured and compared to simulations, see Figure 6

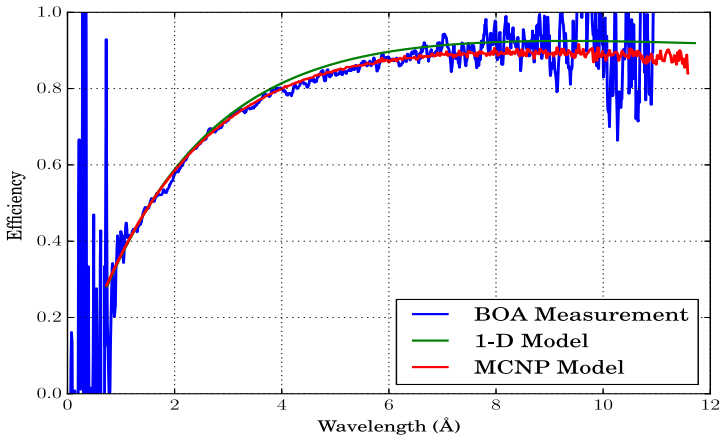


*Figure 6: Comparison between detector efficiency simulated using MCNP and measured at the BOA beamline*

**Deliverable 8.5 - Simulating laminate shielding concepts (ESS-Bilbao)**

In the Deliverable D8.5 report, ESS-Bilbao document a simplistic model approach for simulating multispectral neutron transport through 'slabs' of material. In a simplified geometry, a neutron source using 22 energy-groups in the range meV-GeV are transported through a slab of material. Nine typically used materials from the nuclear industry and neutron scattering are studied, see Table 1 below.

| Material Name | Density |
|---|---|
| Concrete | 2.3 g/cc |
| Carbon Steel | 7.85 g/cc |
| Lead | 11.35 g/cc |
| Concrete with Baryum | 3.35 g/cc |
| Boron Carbide | 2.5 g/cc |
| High density concrete | 3.6 g/cc |
| Borated paraffin | 1.04 g/cc |
| Tungsten powder in paraffin wax | 11.4 g/cc |
| Concrete with Ba/B/Fe | 4.99 g/cc |

*Table 2: Materials studied in the Deliverable 8.5 report*

Based on the systematic findings, a spreadsheet-method has been defined, allowing simplified and realistic estimation of the performance of multi-layered shielding. The results allow to estimate the

performance of relatively complex shielding with a mere spreadsheet with significant accuracy. While the results certainly do not have the power of a full-blown Monte-Carlo or deterministic simulation, they serve as an initial point to start optimizing the shielding and look into the particularities of each problem.

**Work in progress toward Deliverable 8.6**

At the ESS a new polyethylene-$B_4C$ based shielding-concrete has been developed and characterised, see D.D. DiJulio et. al *"A polyethylene-B4C based concrete for enhanced neutron shielding at neutron research facilities"* in NIM A ***859****, 1 July 2017, pp. 41–4*6 (copy of accepted manuscript also available at https://arxiv.org/abs/1703.03713).

The main findings of this publication are that with respect to a "standard" concrete, the newly developed concrete has a 15% lower mass density, a compressible strength of 50% and has an improved shielding performance in MeV range neutrons. It is further reported that the experimental findings are reproduced by Geant4-simulations.

Further characterization studies of the concrete includes a fire test, which can be found in the ESS technical report ESS-0096709. With respect to normal concrete that has an "A" fire safety rating, the developed PE-$B_4C$-concrete has "B-s1,d0" status where which classifies the concrete as 'acceptable' for fire safety.

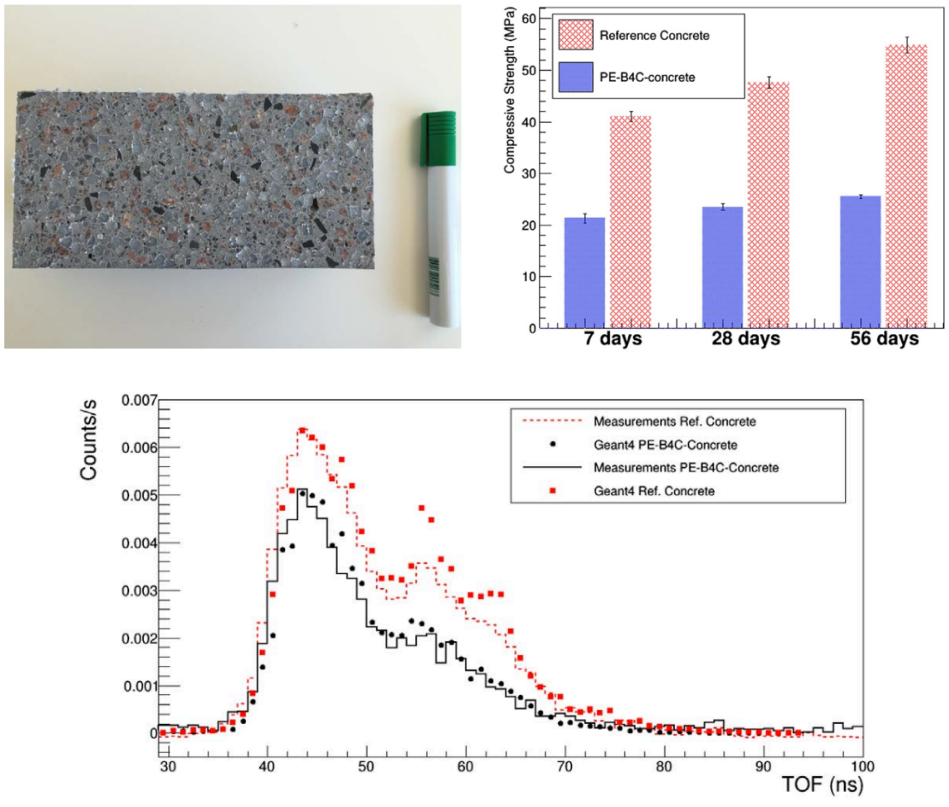


*Figure 7: reproduced from D.D. DiJulio et. al. Top left: Photo of a cross-section of PE-B4C-concrete, the marker is shown for reference. Top right: The compressive strength of the reference concrete and PE-B4C-concrete after 7, 28 and 56 setting days.*

*Bottom: A comparison of transmission-measurements and corresponding (Geant4) simulations for a reference concrete and the developed PE-B4C-concrete.*

**Work in progress on concrete activation – toward Deliverable 8.16 and 8.17** (MTA-EK, DTU)

MTA-EK has been performing an X-ray fluorescence (XRF) study to compare the detailed elemental composition of the ESS-developed PE-$B_4C$ concrete and a standard concrete. As seen in Table 3 below, some variation was found wrt. the *reference* composition as supplied from the concrete manufacturer.

Further, an MCNP- and CINDER'90 based simulation study of how the two concretes should be affected by irradiation at the BNC reactor were performed in collaboration with DTU: Expected neutron fluxes in the BNC irradiation channels were estimated using MCNP, after which the expected time-dependent radionuclide activities for the two nominal and XRF-measured material compositions were estimated using the CINDER'90 nuclear inventory code. Figure 8 below shows how the activation is expected to decay after one week of irradiation and one week of cooling.

The simulated concrete activation studies were presented in a poster at the ICANS 2017 meeting, and will further will become available as a paper in the ICANS proceedings.

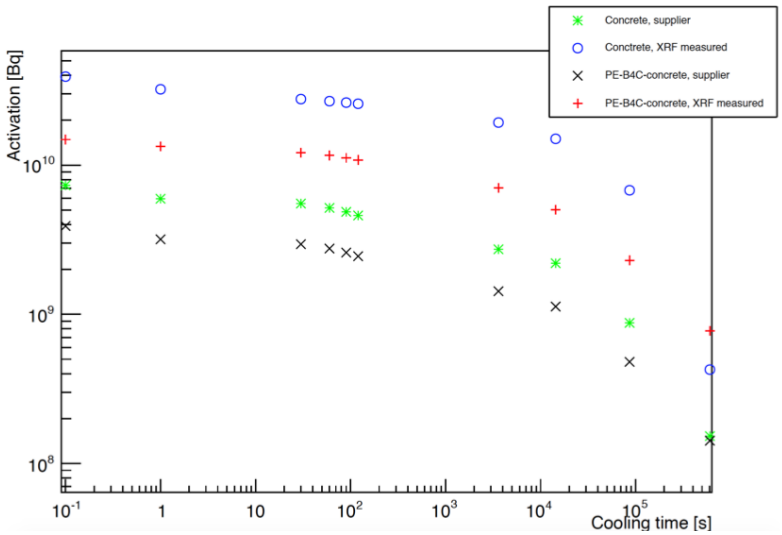


*Figure 8: Simulated activity of PE-$B_4C$-concrete and reference concrete with the XRF-measured and the nominal composition (one week of irradiation followed by one week of cooling)*

Irradiation experiments on PE-B4C concrete, standard concrete, and typical metal components of shielding are now started at BRR Budapest Research Reactor, the first set of samples were irradiated in June 2017.

| | Concrete | | | PE-B4C-Concrete | | | |
|---|---|---|---|---|---|---|---|
| | Reference | Polarized XRF Epsilon5 Average | St Dev | Reference | Polarized XRF Epsilon5 Average | St Dev | Limit of Detection |
| **Matrix wt%** | | | | | | | |
| $B_4C$ | | | | 0.760 | 11.025 | 1.533 | |
| PE | | | | 10.200 | | | - |
| **Major elements wt%** | | | | | | | |
| Na | 1.060 | 1.968 | 0.197 | 0.617 | 1.291 | 0.197 | 0.281 |
| Mg | 0.237 | 0.953 | 0.295 | 0.196 | 0.983 | 0.295 | 0.116 |
| Al | 3.700 | 6.656 | 0.036 | 2.350 | 5.512 | 0.036 | 0.250 |
| Si | 32.700 | 30.098 | 0.003 | 28.600 | 27.037 | 0.003 | 0.223 |
| P | 0.045 | < LOD | - | 0.026 | 0.000 | 0.000 | 0.050 |
| S | 0.236 | 0.169 | 0.015 | 0.278 | 0.237 | 0.015 | 0.009 |
| K | 2.120 | 2.190 | 0.001 | 1.260 | 1.947 | 0.001 | 0.002 |
| Ca | 7.120 | 6.634 | 0.000 | 8.100 | 8.543 | 0.000 | 0.002 |
| Fe | 1.160 | 1.343 | 0.001 | 1.160 | 1.467 | 0.001 | 0.001 |
| **Trace elements ppm** | | | | | | | |
| Cl | 30.0 | | | 35.5 | 130.0 | 10.0 | 30.0 |
| Sc | | 14.3 | 2.1 | | 11.8 | 3.4 | 6.8 |
| Ti | 910.0 | 1760.0 | 10.0 | 520.0 | 1590.0 | 10.0 | 10.0 |
| V | | 55.5 | 0.2 | | 57.6 | 7.1 | 7.1 |
| Cr | | 44.3 | 0.3 | | 82.2 | 1.3 | 2.3 |
| Mn | | 230.0 | 0.0 | | 230.0 | 10.0 | 10.0 |
| Co | | 32.2 | 2.2 | | 61.1 | 1.5 | 1.2 |
| Ni | | 6.4 | 0.7 | | 11.7 | 0.8 | 1.2 |
| Cu | | 22.4 | 0.5 | | 43.5 | 0.6 | 0.7 |
| Zn | | 87.7 | 0.5 | | 100.1 | 0.9 | 0.7 |
| Ga | | 10.9 | 0.6 | | 7.8 | 0.4 | 0.8 |
| Ge | | 3.2 | 0.2 | | 4.9 | 0.3 | 1.3 |
| As | | < LOD | - | | 2.9 | 0.1 | 1.3 |
| Se | | < LOD | - | | 0.0 | 0.0 | 1.3 |
| Rb | | 76.0 | 0.7 | | 59.4 | 0.4 | 0.4 |
| Sr | | 380.9 | 1.3 | | 311.7 | 1.2 | 0.4 |
| Y | | 12.3 | 0.4 | | 11.6 | 0.2 | 0.7 |
| Zr | | 114.1 | 0.8 | | 91.4 | 0.4 | 0.7 |
| Nb | | 6.2 | 0.1 | | 5.4 | 0.1 | 0.4 |
| Mo | | 2.2 | 0.1 | | 3.0 | 0.1 | 0.4 |
| Ag | | < LOD | - | | < LOD | - | 0.4 |
| Cd | | < LOD | - | | < LOD | - | 0.4 |
| In | | 1.3 | 0.1 | | 1.7 | 0.2 | 0.4 |
| Sn | | 2.8 | 0.3 | | 2.8 | 0.0 | 0.5 |
| Sb | | 1.2 | 0.2 | | 1.6 | 0.2 | 0.5 |
| Cs | | 3.9 | 0.1 | | 2.6 | 0.3 | 0.4 |
| Ba | | 665.1 | 1.6 | | 508.5 | 1.1 | 1.1 |
| La | | 23.7 | 0.3 | | 20.0 | 0.3 | 1.3 |
| Ce | | 37.0 | 7.9 | | 41.2 | 0.5 | 1.5 |
| Pr | | 5.5 | 0.5 | | 4.8 | 0.5 | 2.6 |
| Nd | | 18.6 | 4.3 | | 19.5 | 0.2 | 1.8 |
| W | ground in WC | 111.4 | 0.4 | ground in WC | 164.8 | 0.5 | 0.5 |
| Pb | | 19.4 | 0.4 | | 18.3 | 0.9 | 0.9 |
| Th | | 4.7 | 0.2 | | 3.8 | 0.3 | 0.9 |
| U | | 3.4 | 0.2 | | 2.7 | 0.4 | 0.8 |

*Table 3: Nominal and XRD-determined element composition data from standard concrete and developed PE-B4C concrete.*

**Task 8.3: Compact Instrumentation for Larmor Labelling applications at the ESS** *(Responsible: TU-Delft with observers: DTU, STFC, MTA-EK and ESS)*

This task is investigating possibilities for the implementation of new magnetic field configurations, e.g. triangular coils, which should lead to compact Spin Echo SANS and Larmor diffraction instruments and therefore high brilliance combined with high performance. This will result in new instrument designs for both monochromatic and wide-band (time-of-flight) operation. This development will be of particular relevance to the ESS, where the proposed flat (pancake) moderator design will result in high intensity, small cross-section neutron beams that are well-adapted to small samples and compact instruments.

**Work in progress toward Deliverable 8.7**

A Post Doc was employed in Delft from late 2016 and work is progressing well. The Post Doc presented early material on analytical parameter studies for compact Larmor options at the ICANS 2017 WP meeting.

For example, compact Neutron Spin Echo (NSE) designs require magnetic field inhomogeneity (ΔJ) which is comparable to that in present instruments (with long main coils) to be achieved with a shorter main coil. Therefore, ΔJ-dependence on other instrument parameters (radius of the coil, distances to the flippers) as well as by the beam properties (beam cross-section and divergence) was analyzed in search for a possibly not yet discovered region of parameter space. A cut through this parameter space is shown in Figure 9. The full results will be presented in the upcoming deliverable.

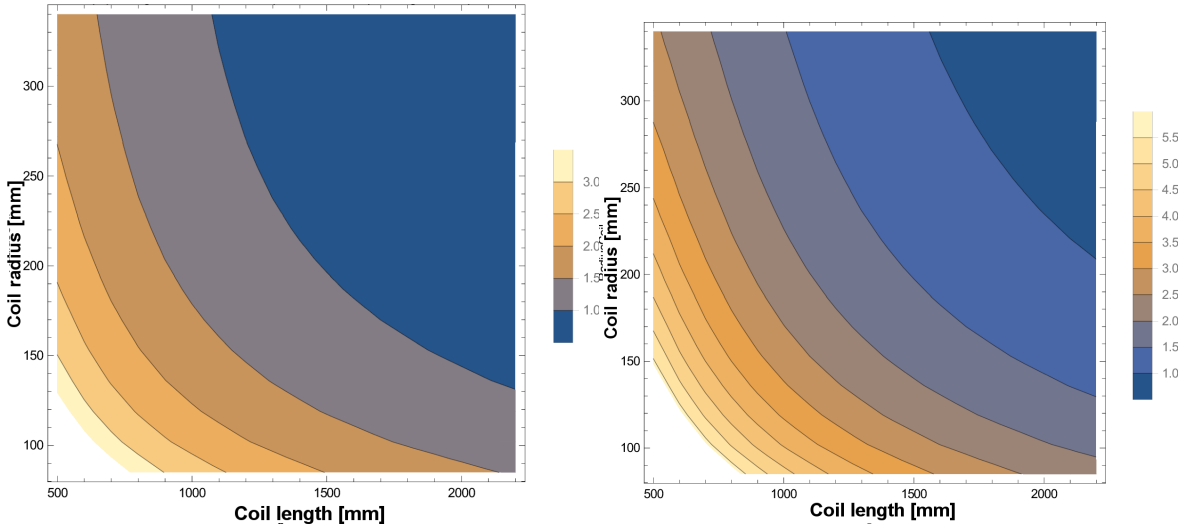


*Figure 9: The magnetic field inhomogenity, ΔJ, a function of coil length and radius, normalized to ΔJ calculated for a main coil similar to that of FZJ-NSE (2 m long, inner radius 17 cm). Calculations were done with RADIA (ESRF) for a homogeneous (left) and divergent (gaussian standard deviation 7 mrad) beam (right).*

Further the first finite-element (FEM) simulations on expected field-strength of the compact magnetic systems were presented, generated using the Infolytica MagNet software. Figure 10 below shows output of such simulations for an RF-flipper system. Such systems could be used for realization of a compact spin-echo module on a SANS instrument. See e.g. the related publication A. Kusmin et . al "Feasibility and applications of the spin-echo modulation option for a small angle neutron scattering instrument at the European Spallation Source" in NIM A **856**, 1 June 2017, pp. 119–132.

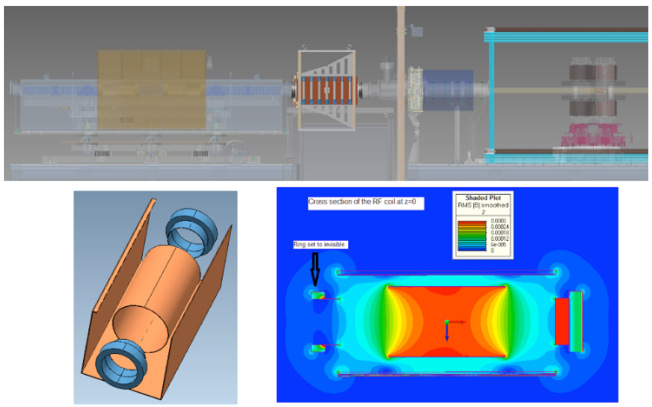

*Figure 10: Illustration of envisioned RF flipper system and related FEM-simulated field strength.*